BIOCHEMISTRY
including biophysical chemistry & molecular biology

Article

pubs.acs.org/biochemistry

Design and Characterization of Chemically Stabilized Aβ42 Oligomers

Ghiam Yamin,[†,§] Tien-Phat Vuong Huynh,[‡] and David B. Teplow*[,§]

[†]Department of Radiology, School of Medicine, University of California, San Diego, California 92093, United States
[‡]Department of Neurology, School of Medicine, Washington University at St. Louis, St. Louis, Missouri 63110, United States
[§]Department of Neurology, David Geffen School of Medicine at UCLA, Los Angeles, California 90095, United States

Supporting Information

ABSTRACT: A popular working hypothesis of Alzheimer's disease causation is amyloid β-protein oligomers are the key neuropathogenetic agents. Rigorously elucidating the role of oligomers requires the production of stable oligomers of each size. We previously used zero-length photochemical cross-linking to allow stabilization, isolation, and determination of structure−activity relationships of pure populations of Aβ40 dimers, trimers, and tetramers. We also attempted to study Aβ42 but found that Aβ42 oligomers subjected to the same procedures were not completely stable. On the basis of the fact that Tyr is a critical residue in cross-linking chemistry, we reasoned that the chemical accessibility of Tyr10 in Aβ42 must differ from that in Aβ40. We thus chemically synthesized four singly substituted Tyr variants that placed the Tyr in different positions across the Aβ42 sequence. We then studied the stability of the resulting cross-linked oligomers as well as procedures for fractionating the oligomers to obtain pure populations of different sizes. We found that [Phe[10],Tyr[42]]Aβ42 produced stable oligomers yielding highly pure populations of dimers through heptamers. This provides the means to establish formal structure−activity relationships of these important Aβ42 assemblies. In addition, we were able to analyze the dissociation patterns of non-cross-linked oligomers to produce a model for oligomer formation. This work is relevant to the determination of structure−activity relationships that have the potential to provide mechanistic insights into disease pathogenesis.

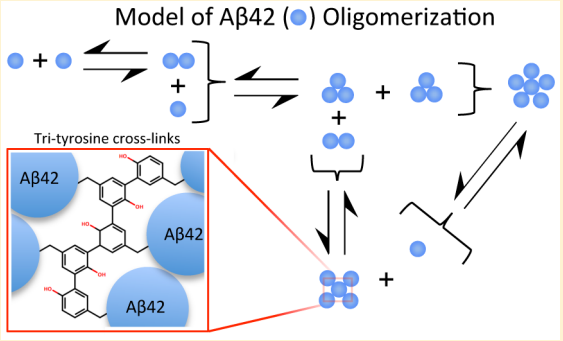

Alzheimer's disease (AD) is a neurodegenerative disorder that causes irreversible damage to the brain that manifests in memory loss, cognitive dysfunction, and eventual death. AD is characterized by the cerebral deposition of plaques composed of aggregated fibrils of the amyloid β-protein (Aβ), a 40−42-amino acid peptide. These aggregates long were believed to be the proximate neurotoxins in AD. However, this idea has been supplanted by the working hypothesis that Aβ oligomers are more relevant etiologic targets.[1−7] Designing therapeutic agents specific for "oligomers" requires establishing accurate structure−neurotoxicity relationships. Unfortunately, Aβ is an intrinsically disordered protein that self-associates to form oligomers that are metastable and polydisperse, factors that largely have prevented formal structure−neurotoxicity studies.

A fruitful approach for stabilizing oligomers of specific size has been zero-length cross-linking using the technique of photoinduced cross-linking of unmodified proteins (PICUP).[8] Oligomers stabilized in this manner do not self-associate or dissociate.[9,10] This has allowed the fractionation and purification of stable Aβ40 oligomers of specific sizes using sodium dodecyl sulfate−polyacrylamide gel electrophoresis (SDS−PAGE).[10] These cross-linked oligomers demonstrated neurotoxic activity similar or more robust than that of non-cross-linked Aβ40 oligomers.[10]

To study the more clinically relevant Aβ42 isoform of Aβ, we subjected monomeric Aβ42 to PICUP, SDS−PAGE, and extraction. We were surprised to observe that, unlike cross-linked oligomers of Aβ40, the Aβ42 oligomers were not fully stable and thus exhibited partial dissociation in subsequent SDS gels. The phenolic side chain of the amino acid Tyr is highly reactive in PICUP chemistry.[8] It can form dityrosine and trityrosine bonds among different Aβ monomers, as well as covalent bonds between Tyr on different closely associated peptide chains and inter- and intramolecular covalent bonds between Tyr and nucleophilic side chains such as that of lysine.[8] *In vitro* and *in silico* studies have revealed significant differences between Aβ40 and Aβ42 in their conformational dynamics, oligomerization, and fibril formation.[9,11] Conformational differences within the respective Aβ monomers must account for these observations, a conclusion suggesting that Tyr in Aβ42, relative to Aβ40, may be less chemically accessible, shielded, or located in a structurally labile position, preventing complete cross-linking and predisposing oligomers produced thereof to dissociate. If so, we reasoned that repositioning a Tyr

Received: March 23, 2015
Revised: July 31, 2015
Published: August 4, 2015

DOI: 10.1021/acs.biochem.5b00318
Biochemistry 2015, 54, 5315−5321

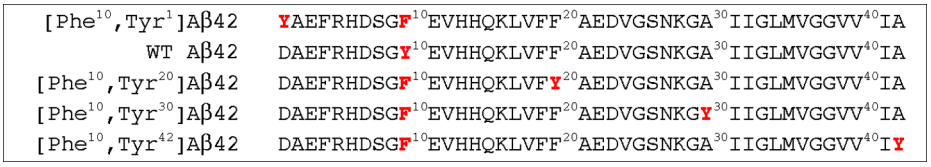

Figure 1. Primary structures of Aβ42 peptides. A Phe residue was substituted for Tyr10 in all peptides except the wild type (WT). Amino acid differences between the WT sequence and those of the other four peptides are colored red.

residue at a different site along the peptide chain could produce more efficient cross-linking. We thus chemically synthesized Aβ42 variants with Tyr substituted at four different locations between the N- and C-termini: Asp1, Phe20, Ala30, and Ala42. We report here the results of studies of the stabilities of these peptides and how these stabilities may be used to model the Aβ42 oligomerization process.

MATERIALS AND METHODS

Chemicals and Reagents. Chemicals were obtained from Sigma-Aldrich and were of the highest purity available. Tris-2,2′-bipyridyl-dichlororuthenium(II) hexahydrate [$Ru(Bpy)_3$], ammonium persulfate (APS), and SimplyBlue SafeStain (Coomassie G-250) were purchased from Invitrogen (Carlsbad, CA). Acrylamide and TEMED were purchased from Bio-Rad (Hercules, CA). *N,N′*-Methylene-bis-acrylamide was purchased from Sigma-Aldrich (St. Louis, MO). All solutions were prepared in double distilled deionized (DDI) water produced from a Milli-Q system (Millipore Corp., Bedford, MA).

Peptide Design and Synthesis. Aβ42 peptides were synthesized using 9-fluorenylmethoxycarbonyl (Fmoc) chemistry, purified by reverse phase high-performance liquid chromatography, and characterized by mass spectrometry and amino acid analysis, as described previously.[12] Quantitative amino acid analysis and mass spectrometry yielded the expected compositions and molecular weights, respectively, for each peptide (see Figure 1 for peptide sequences). Tyr10 was replaced with Phe in each of the four Aβ42 variants. This was done to prevent intramolecular cross-linking and multipoint intermolecular cross-linking, each of which would complicate the analysis of cross-linking patterns. We have shown in previously published work that the Tyr10Phe substitution does not alter the oligomerization process.[13] Purified peptides were stored as lyophilizates at −20 °C.

Preparation of Aβ Solutions. Stock solutions of Aβ were prepared by reconstituting the lyophilized peptide in a 1:4.5:4.5 (v/v/v) mixture of 60 mM NaOH, Milli-Q water, and 22.2 mM sodium phosphate (pH 7.5) to yield a nominal Aβ concentration of 1 mg/mL in 10 mM sodium phosphate (pH 7.5). The peptide solution then was sonicated for 1 min in a bath sonicator (model 1510, Branson, Danbury, CT) and filtered through a 30 kDa molecular weight cutoff Microcon centrifugal filter device (Millipore, Billerica, MA) for 15 min at room temperature (RT, 22 °C) at 16000*g*. The filtrate was collected, and the Aβ concentration was determined by UV absorbance (ε_{280} = 1280 cm^{-1} M^{-1}) using a 1 cm quartz cuvette (Hellma, Plainview, NY) and a Beckman DU-640 spectrophotometer (Beckman Instruments, Fullerton, CA). All measurements were performed at RT. This protocol results in uniform and reproducible material termed low-molecular weight (LMW) Aβ.[14]

Cross-Linking, SDS−PAGE, and Gel Staining. Peptides were covalently cross-linked using the technique of photo-induced cross-linking of unmodified proteins (PICUP) immediately after LMW Aβ preparation.[15] Briefly, 3 μL of 2 mM $Ru(Bpy)_3$ and 3 μL of 40 mM APS were added to 54 μL of 80 μM Aβ42 (or its analogues) in 10 mM sodium phosphate buffer (pH 7.5). The final Aβ:$Ru(Bpy)_3$:APS molar ratio was 0.72:1:20. The mixture was irradiated for 1 s with a "Fiber-Lite" high-intensity visible light source (Dolan-Jenner, Boxborough, MA), and the reaction was immediately quenched with 1 μL of 1 M dithiothreitol (DTT) in 10 mM sodium phosphate buffer (pH 7.4). For each reaction, APS and $Ru(Bpy)_3$ were added to the Aβ solution and the mixture was vortexed for 1 s after addition of the cross-linking reagents and immediately preceding irradiation. Two cross-linking reactions typically were done to produce a total volume of 122 μL.

For SDS−PAGE analysis, the 122 μL of cross-linked Aβ was mixed with 122 μL of 2× Tricine sample buffer (Invitrogen). Two hundred microliters of this cross-linked oligomer mixture was boiled for 10 min and then introduced into a modified Novex 10−20% Tricine gel (1.0 mm × 10 wells) (Invitrogen). The gel was modified by using a scalpel to remove eight of the nine "teeth" at the top of the stacking gel. This produced two lanes from the original 10, one with a width of ≈7.0 cm and one remaining original well with a width of ≈0.8 cm. The cross-linked oligomer mixture was pipetted into the large lane. Molecular weight markers were pipetted into the small lane.

After SDS−PAGE, gels were washed in water three times for 5 min each and then incubated in SimplyBlue SafeStain (Invitrogen) overnight on a ZD-9556 orbital shaker (Madell Technology, Ontario, CA) rotating at 60 rpm. The next morning, the gel was destained for 30 min and then incubated again with fresh SimplyBlue SafeStain for 2 h. Afterward, the gel was destained for 30 min in DDI water. Bands were excised using a scalpel blade (Fisher, Pittsburgh, PA) and placed in individual 1.5 mL microcentrifuge tubes.

Modified "Cleveland Gel" System and Densitometry Analysis. Gel pieces corresponding to each respective oligomer band excised from the preparative 10−20% acrylamide gel were re-electrophoresed in a second, larger gel using the Protean IIxi Cell Gel System (Bio-Rad), similar to the procedure of Cleveland et al.[16] that is used for the separation of peptide fragments produced from gel slices treated with proteases *in situ* in polyacrylamide gel wells prior to electrophoresis. The gels were 1.5 mm in thickness, which accommodated the thickness of the excised gel pieces from the 1.0 mm Novex 10−20% Tricine gel. The gels were made with an 18% T resolving polyacrylamide gel and a 4% T acrylamide stacking gel, which provided the optimal separation of the extracted oligomers. A 20-well comb was inserted into the stacking gel during polymerization. Afterward, the comb was removed and a scalpel was used to carefully excise the acrylamide gel between every other pair of wells to create nine larger wells [except for the first well, which was used for the MW marker (MWM)]. Excised gel pieces containing the respective oligomers were boiled in 200 μL of 2× Novex Tricine SDS sample buffer (Invitrogen) for 10 min and then

DOI: 10.1021/acs.biochem.5b00318
Biochemistry 2015, 54, 5315−5321

placed into individual lanes. An additional 30 μL of this same buffer then was added to each lane. Finally, Mark12 Unstained Standard (Invitrogen) MWM was added to the MWM well. To allow for better resolution and prevent overheating, the gel was run at 4 °C at 50 V for 5 h and then the voltage was increased to 80 V for 15−20 h. The gel was silver-stained using a Silver-Xpress silver staining kit (Invitrogen) and scanned with a Canon CanoScan 9950 flatbed scanner. Gel images were converted to 256 grayscale and analyzed using ImageJ version 1.43r (http://imagej.nih.gov/ij/) to produce intensity profiles. To correct for overlapping peaks, the intensity profiles were imported into Magicplot Student version 2.0.1 (http://magicplot.com/), where nonlinear curve fitting allowed overlapping peaks to be deconvoluted into individual peaks, assuming each peak was Gaussian in nature. The relative intensities were calculated on the basis of the integration of the area under each fitted curve after baseline correction. Individual peak values were normalized to the total intensity within each lane. The data then were plotted using Kaleidagraph version 4.0.4 (Synergy Software, Reading, PA).

RESULTS

Oligomer Size Distributions of Wild-Type (WT) Aβ42 and Its Tyr-Substituted Variants. We chemically synthesized Aβ42 variants with Tyr substituted at four different locations between the N- and C-termini: Asp1, Phe20, Ala30, and Ala42. To preclude intramolecular cross-linking occurring through the WT Tyr10 residue, we replaced this residue with Phe (Figure 1). We then determined how the movement of Tyr across the Aβ42 peptide affected oligomerization, as monitored using PICUP, SDS−PAGE, and silver staining (Figure 2). In the absence of cross-linking, Aβ42 and its four Tyr variants produced bands electrophoresing predominantly at monomer and trimer (filled white arrowheads). Less intense tetramer bands also were observed (empty white arrowheads). These trimer and tetramer bands previously have been shown to be SDS-induced artifacts.[9] [Phe10,Tyr20]Aβ42 produced few SDS-stable oligomers. The predominant band was the monomer band, while only a faint trimer band (filled white arrowhead) was observed. The other four peptides all displayed tetramer bands, of which the tetramer band from [Phe10,Tyr42]Aβ42 was the most prominent (Figure 2, empty arrowheads).

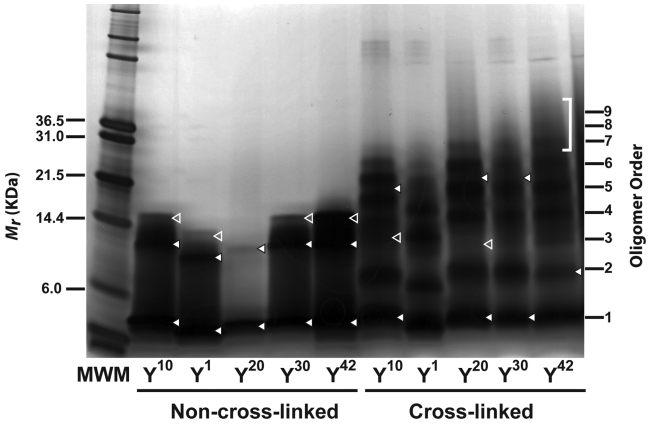

Figure 2. Oligomer size distributions of WT Aβ42 and its Tyr-substituted variants. PICUP, SDS−PAGE, and silver staining were used to determine oligomer size distributions. Eight microliters of 40 μM peptide were loaded into each well, corresponding to 1.44 μg for the Aβ42 lanes and 1.47 μg for the [Phe10,Tyr42]Aβ42 lanes. Abbreviations: MWM, molecular weight marker; M_r, relative molecular mass in daltons; $Y^{\#}$, position of the Tyr in each respective peptide. Y^{10} signifies WT Aβ. Peptides were prepared and immediately electrophoresed ("non-cross-linked"), or they were prepared, immediately cross-linked, and then electrophoresed ("cross-linked"). Arrowheads and bracket refer to specific bands (see the text). Trimer and tetramer bands in the lanes of un-cross-linked are SDS-induced artifacts.[9] The starting material is aggregate-free.

Cross-linked WT Aβ42 produced eight bands corresponding to monomer through heptamer, with nodes at monomer and pentamer/hexamer (filled white arrowheads). [Tyr1,Phe10]-Aβ42 produced a similar distribution, but with band mobilities shifted toward lower M_r values (relative molecular mass). These shifts also were observed in the non-cross-linked control. [Phe10,Tyr20]Aβ42 produced seven bands, corresponding to monomer through heptamer, with nodes at monomer and pentamer/hexamer (filled white arrowheads). The trimer band (empty white arrowhead) was fainter than those of the other oligomers. [Phe10,Tyr30]Aβ42 displayed a pattern of bands similar to that of WT Aβ42 (filled white arrowheads). [Phe10,Tyr42]Aβ42 behaved differently. The amount of dimer (filled white arrowhead) was smaller than those of the other peptides, and the amounts of heptamer, octamer, and nonamer were larger (white bracket). It appeared that Tyr substitutions closer to the C-terminus produced larger amounts of higher-order[a] oligomers.

Stability of Cross-Linked Oligomers. To determine whether cross-linked Aβ42 oligomers were covalently associated, we performed PICUP reactions and fractionated the resulting products by SDS−PAGE. We excised bands identified by Coomassie Blue staining and then re-electrophoresed their component peptides by placing the gel pieces in wells of a second SDS gel. We predicted that bands containing covalently associated oligomers should "run true" when re-electrophoresed, i.e., with an M_r identical to that in the original gel. Noncovalently associated oligomers, or oligomers that were not cross-linked completely, would produce multiple bands migrating at or below their initially observed M_r values.

We made four observations in experiments using WT Aβ42 (Figure 3a): (1) an order-dependent ladder of bands, (2) cross-linked oligomers of order 2−7 that were unstable, (3) unstable oligomers that produced lower-order species varying in size from 1 to 6 (as predicted), and (4) bands of M_r higher than the M_r values of the originally isolated bands that were observed. We quantified band intensities and then normalized these intensities for each lane (Figure 3b and Table S1). These data showed that the most intense band in each lane corresponded to the M_r of the band excised from the first SDS gel. The purest oligomer was dimer (67%). The least pure oligomer was tetramer (28%). In addition, relative to oligomers of order 2−5, purified hexamers and heptamers appeared more stable.

We next performed identical experiments using the four Tyr variants, [Tyr1,Phe10]Aβ42 (Figure S1 and Table S2), [Phe10,Tyr20]Aβ42 (Figure S2 and Table S3), [Phe10,Tyr30]-Aβ42 (Figure S3 and Table S4), and [Phe10,Tyr42]Aβ42 (Figure 4 and Table S5). We observed behavior similar to that of WT Aβ42 for the first three peptides (summarized in Table 1). In contrast, the [Phe10,Tyr42]Aβ42 peptide was exceptionally stable (cf. Figures 3 and 4 and Tables S1 and S5). The lowest purity observed was 75% (tetramer), compared with 28% for WT Aβ42. Similarly, the most stable WT Aβ42 oligomer, dimer, was 67% pure, whereas the equivalent

DOI: 10.1021/acs.biochem.5b00318
Biochemistry 2015, 54, 5315−5321

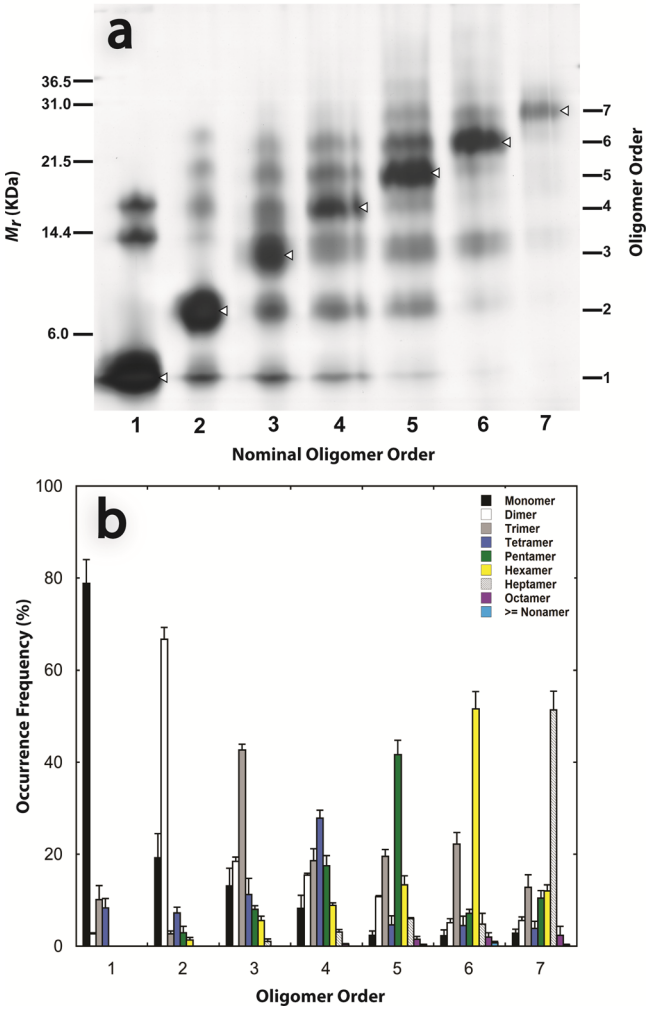

Figure 3. WT Aβ42 oligomer stability. Aβ42 was cross-linked and then electrophoresed in an SDS gel (see Materials and Methods). (a) Coomassie-stained oligomer bands were excised and re-electrophoresed, and the resulting bands visualized by silver staining. Each lane number represents the expected oligomer order. (b) ImageJ and MagicPlot were used to determine the occurrence frequencies of oligomers of each order. Data are representative of at least three independent experiments.

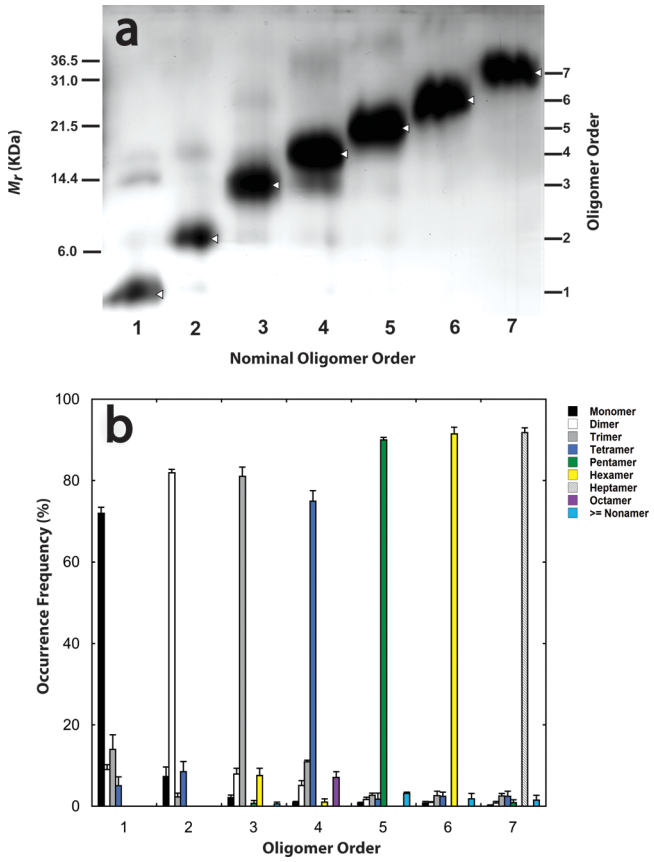

Figure 4. [Phe10,Tyr42]Aβ42 oligomer stability. [Phe10,Tyr42]Aβ42 was cross-linked and then electrophoresed in an SDS gel (see Materials and Methods). (a) Coomassie-stained oligomer bands were excised and re-electrophoresed, and the resulting bands visualized by silver staining. Each lane number represents the expected oligomer order. (b) ImageJ and MagicPlot were used to determine the occurrence frequencies of oligomers of each order. Data are representative of at least three independent experiments.

oligomer produced by [Phe10,Tyr42]Aβ42 was 82% pure. As suggested earlier, the higher-order oligomers were most stable. Pentamers, hexamers, and heptamers were all >90% pure. In some experiments, octamers and higher-order oligomers also were observed in relatively pure form.

Are "Stable" Aβ42 Oligomers Really Stable? Our prior experiments showed that replacing Ala42 with Tyr produced a peptide that produced cross-linked oligomers of exceptional stability. Nevertheless, we sought to subject these ostensibly stable oligomers to an additional denaturation/dissociation procedure to convince ourselves of their stability. To do so, we re-electrophoresed purified oligomers a second time (a total of three SDS gels). We performed identical experiments with WT Aβ42 so that we could compare the stabilities of the oligomers formed by each peptide (Table 2). It is clear from inspection (cf. Figures S4 and S5) that the [Phe10,Tyr42]Aβ42 peptide produced exceptionally stable oligomers. The purity of each oligomer was significantly greater than that of the corresponding oligomer formed by WT Aβ42, with the exception of trimer (87% for [Phe10,Tyr42]Aβ42 vs 90% for WT Aβ42) (Tables S6 and S7). Lower- and higher-order species were observed with WT Aβ42, suggesting some instability of the purified oligomers (Figure S4). In contrast, only faint dimer and trimer bands were observed in the tetramer and pentamer lanes with [Phe10,Tyr42]Aβ42 oligomers (Figure S5).

DISCUSSION

Formation of toxic Aβ42 oligomers is thought to be a seminal neuropathogenetic process in AD.[17,18] If so, then design of oligomer-specific therapeutic agents requires the determination of structure−activity relationships (SAR) among the different types of oligomers. Unfortunately, the metastability and polydispersity of oligomer preparations have complicated this determination. The experiments conducted in this study demonstrate that positioning of a single Tyr residue at position 42 within Aβ42 allows the production and isolation of highly stable, pure populations of Aβ42 oligomers following photochemical cross-linking using the technique of PICUP.

Previous studies have shown that PICUP is capable of revealing the distribution of Aβ oligomers present in an equilibrium state in which rapid association and dissociation reactions occur. These distributions were not stochastic; i.e., they did not represent distributions created by diffusion-limited

DOI: 10.1021/acs.biochem.5b00318
Biochemistry 2015, 54, 5315−5321

Table 1. Oligomer Stabilities of Cross-Linked WT Aβ42 and Aβ42 Tyr Variants after Cleveland Gel Isolation[b]

	oligomer order							
peptide	1	2	3	4	5	6	7	8
WT Aβ42	79 ± 5	67 ± 3	43 ± 1	28 ± 2	42 ± 3	52 ± 4	51 ± 4	N/A
[Y1,F10]Aβ42	93 ± 1	74 ± 3	36 ± 8	28 ± 5	43 ± 6	36 ± 1	52 ± 8	N/A
[F10,Y20]Aβ42	74 ± 3	64 ± 5	34 ± 6	41 ± 2	50 ± 2	63 ± 2	60 ± 2	N/A
[F10,Y30]Aβ42	79 ± 2	75 ± 7	46 ± 5	51 ± 4	71 ± 3	77 ± 3	76 ± 2	N/A
[F10,Y42]Aβ42	72 ± 2	82 ± 1	81 ± 2	75 ± 3	90 ± 1	92 ± 2	92 ± 1	N/A

[b]Values are the percentage ± the standard deviation.

Table 2. Oligomer Stabilities of Cross-Linked WT Aβ42 and [Phe10,Tyr42]Aβ42 after Two Consecutive Cleveland Gel Isolations[b]

	oligomer order							
peptide	1	2	3	4	5	6	7	8
WT Aβ42	96 ± 2	90 ± 2	90 ± 2	61 ± 5	59 ± 5	57 ± 4	64 ± 5	83 ± 2
[F10,Y42]Aβ42	96 ± 0.7	96 ± 1.4	87 ± 0.4	83 ± 3	91 ± 2.3	92 ± 1.3	92 ± 3	N/A

[b]Values are percentages ± the standard deviation.

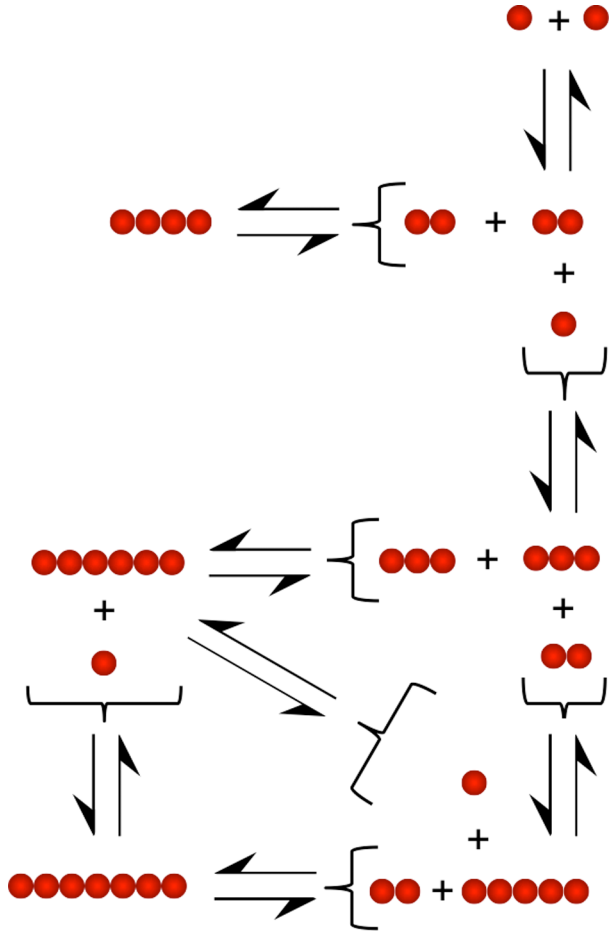

Figure 5. Model of Aβ42 oligomerization. The association and dissociation patterns observed for oligomer orders 2−7 (Figures 2−4 and Figures S1−S3), along with the occurrence frequencies for each oligomer (Tables S1−S5), were used to produce a model of oligomer formation. Simple monomer addition models, akin to actin polymerization,[30] do not appear to explain these data. Instead, key roles are played by monomers, dimers, and trimers, which appear to act as building blocks for higher-order oligomers.

monomer collisions.[19] This question was addressed experimentally and theoretically.[20] Briefly, the PICUP-generated oligomer distributions of two amyloidogenic [Aβ and human calcitonin (CT)] and two nonamyloidogenic [human pituitary adenylate cyclase-activating polypeptide (PACAP) and human growth hormone-releasing factor (GRF)] peptides, all of similar molecular weight, were compared. We reasoned that amyloidogenic peptides, which are known to self-associate rapidly, should produce oligomer distributions reflective of the pre-existence of oligomers prior to execution of the cross-linking chemistry. In contrast, the nonamyloidogenic peptides would be expected to produce oligomer distributions reflective of oligomerization caused almost solely by diffusion-limited monomer collisions. These latter distributions would look like simple ladders, containing one node of intensity dependent on diffusion rates and peptide concentration. The former distributions would be distinct from those of the latter and could contain multiple nodes. This was what we observed.[9,20] We also modeled the distributions mathematically by parameterizing a simple diffusion-limited collisional oligomerization model with peptide concentration and chemical reactivity (efficiency). These distributions (see Figure 6 of ref 20) were contrasted with that obtained for Aβ40, revealing that the latter distribution was distinct and therefore could not be explained by diffusion-limited collisions of the monomer. The distributions also did not represent distributions obtained by partial cross-linking of much larger oligomers, as such oligomers were not found to exist.[20] Instead, the distributions comprised predominately oligomers of order 2−7 that preexisted in solution. The data thus supported the conclusion that the PICUP chemistry produced accurate insights into oligomer distribution.

Data supporting the relevance of cross-linked species to analyses of biophysical and neurotoxic properties of oligomers also have come from the salmon calcitonin amyloid system.[21,22] Salmon calcitonin (sCT), like Aβ, appears to be intrinsically disordered but capable of forming oligomers and α-helix-containing assembly intermediates. The α-helical state is relatively stable, which may explain why sCT fibril formation is a slow process. However, this fact has provided an opportunity to compare the oligomerization distributions of PICUP-cross-linked and non-cross-linked (native) sCT using SDS−PAGE.[21] The two distributions are highly similar, comprising predominately dimers and trimers, but each of

DOI: 10.1021/acs.biochem.5b00318
Biochemistry 2015, 54, 5315−5321

these species is enriched after cross-linking. These data support the conclusion that cross-linking does not substantially alter the oligomerization or electrophoretic properties of the peptide but simply stabilizes the oligomers against dissociation. The implication is that structure−activity relationships established in neurotoxicity experiments with cross-linked sCT are likely to reflect the same SAR established with non-cross-linked material. Induction suggests that cross-linked Aβ oligomers thus would behave like their non-cross-linked structural homologues, although this cannot formally be proven with current techniques.

Our experiments suggest, on average, that the stability of cross-linked oligomers increases as the Tyr is moved from the N-terminus to the C-terminus. This was especially true for oligomers of an order greater than trimer, for which the purity of [Phe10,Tyr42]Aβ42 tetramer through heptamer was 75−92%, a range significantly higher than that for the other peptides (e.g., [Tyr1,Phe10]Aβ42 had a range of 28−74%). The replacement of Ala42 with Tyr increases the hydrophobicity of the Aβ42 C-terminus, an effect that has been shown to facilitate formation of higher-order oligomers (n > 7).[19] This substitution also would be expected to stabilize a C-terminal turn in Aβ42 that is critical for oligomer stability.[23] We previously showed that Tyr substitution at residue 30 or 42 significantly diminishes its intrinsic fluorescence relative to substitution at position 1, 10, or 20, a result suggesting stabilization or shielding of the Tyr.[24] Measurements of solvent accessible surface areas using molecular dynamics simulations are consistent with Tyr shielding at the C-terminus.[25] These studies also revealed that Aβ42 oligomer formation was predominantly driven by intermolecular interactions among the C-terminal regions. The stabilization within the C-terminus may play an important role in the oligomerization process and explain the rapid evolution of later assembly states such as protofibrils and fibrils. This suggests a simple mechanism by which the Tyr42 substitution leads to stably cross-linked oligomers—it maintains the Aβ42 monomers comprising the various oligomers in conformations amenable to rapid intermolecular cross-linking. In the absence of such structural stabilization, rapid conformational fluctuations in Aβ preclude the Tyr−Tyr interactions necessary for cross-linking during the short time span of the reaction (≈1 s). It is interesting in this regard that recent studies of oligomers have used increased irradiation times (7−10 s) to perform the PICUP chemistry.[26,27]

We note that [Tyr1,Phe10]Aβ42 formed the least stable oligomers. It may be relevant in this regard that this peptide displayed a distinct oligomerization pattern relative to those of the other four peptides. All [Tyr1,Phe10]Aβ42 oligomer bands displayed lower M_r values, and the intensities of the pentamer and hexamer bands were relatively low. The anomalous migration of [Tyr1,Phe10]Aβ42 oligomers may be due to oligomer compaction,[13] which could decrease cross-linking efficiency by stabilizing Tyr1 in a conformer that was less able to interact intermolecularly with other Aβ monomers. This phenomenon would be the mirror image of that operating in the [Phe10,Tyr42]Aβ42 system, in which C-terminal collapse contributed to stabilization of a conformer that could cross-link efficiently.[25]

Intrinsic to our discussion of primary structure and oligomer stability (cross-linking efficiency) is the conformational space of each peptide system; i.e., what is the occupation frequency of each volume of that space? In simple terms, for how long does each of the many possible monomer and higher-order conformers exist? The answer to this question is related directly to the energies of formation of each conformer, which directly yield the probability that the particular conformer forms. For Aβ40 and Aβ42, we have addressed this question computationally,[28] and from the probabilities thus obtained, we have been able to construct surfaces that allow direct visualization of the conformational spaces of each peptide. However, this question also can be addressed in the opposite manner, namely by starting with oligomer occurrence frequencies and then constructing models of each conformer. The matrices of nominal oligomer order versus oligomer frequency (Tables S1−S5) provide us the means to do so, as illustrated in Figure 5.

The results of this analysis suggest that the formation of oligomers of order ≤7 occurs predominately through association of dimers and trimers (Figure 5), as opposed to actin-type iterative monomer addition.[29,30] This oligomerization mechanism explains the proclivity of Aβ42 to form paranuclei (pentamers and hexamers). Our suggestions are consistent with results of ion mobility spectrometry studies of Aβ oligomerization, which reveal oligomer distributions without the necessity for chemical cross-linking, that show that Aβ42 readily forms dimers, tetramers, hexamers, and dodecamers.[31,32] Formation of tetramers and hexamers appears to occur by association of dimers and trimers, respectively, as opposed to dimer and monomer association. Of course, production of odd-numbered oligomer units must require addition of monomers. Further studies will be necessary to determine the veracity of these suggestions.

■ ASSOCIATED CONTENT

Supporting Information

The Supporting Information is available free of charge on the ACS Publications website at DOI: 10.1021/acs.biochem.5b00318.

Occurrence frequencies of oligomers of a specific order produced from WT Aβ42 and its four singly substituted Tyr variants (Tables S1−S5) and occurrence frequencies of WT and [Phe10,Tyr42]Aβ42 oligomers of a specific order, analyzed following two consecutive Cleveland gels (Tables S6 and S7, respectively) (PDF)

Oligomer stability of [Tyr1,Phe10]Aβ42 (PDF)

Oligomer stability of [Phe10,Tyr20]Aβ42 (PDF)

Oligomer stability of [Phe10,Tyr30]Aβ42 (PDF)

Stability of WT Aβ42 oligomers after two consecutive Cleveland gel procedures (PDF)

Stability of [Phe10,Tyr42]Aβ42 oligomers after two consecutive Cleveland gel procedures (PDF)

■ AUTHOR INFORMATION

Corresponding Author

*E-mail: dteplow@mednet.ucla.edu.

Author Contributions

G.Y. and T.-P.V.H. contributed equally to this work.

Funding

We gratefully acknowledge support from the UCLA Medical Scientist Training Program (MSTP) (G.Y.), the UCLA Chemistry-Biology Interface (CBI) Training Program (G.Y.), National Institutes of Health Grants NS038328 (D.B.T.), AG027818, and AG041295 (D.B.T.), and the Jim Easton

DOI: 10.1021/acs.biochem.5b00318
Biochemistry 2015, 54, 5315−5321

Consortium for Drug Discovery and Biomarkers at UCLA (D.B.T.).

Notes

The authors declare no competing financial interest.

■ ACKNOWLEDGMENTS

We thank Margaret Condron for synthesizing and purifying the peptides used in this study.

■ ADDITIONAL NOTE

[a]"Order" refers to the number of Aβ monomers comprising any assembly.

■ REFERENCES

(1) Haass, C., and Selkoe, D. J. (2007) Soluble protein oligomers in neurodegeneration: lessons from the Alzheimer's amyloid β-peptide. *Nat. Rev. Mol. Cell Biol. 8*, 101−112.

(2) Dodart, J. C., Meziane, H., Mathis, C., Bales, K. R., Paul, S. M., and Ungerer, A. (1999) Behavioral disturbances in transgenic mice overexpressing the V717F β-amyloid precursor protein. *Behav. Neurosci. 113*, 982−990.

(3) Hsia, A. Y., Masliah, E., McConlogue, L., Yu, G. Q., Tatsuno, G., Hu, K., Kholodenko, D., Malenka, R. C., Nicoll, R. A., and Mucke, L. (1999) Plaque-independent disruption of neural circuits in Alzheimer's disease mouse models. *Proc. Natl. Acad. Sci. U. S. A. 96*, 3228−3233.

(4) Moechars, D., Dewachter, I., Lorent, K., Reverse, D., Baekelandt, V., Naidu, A., Tesseur, I., Spittaels, K., Haute, C. V., Checler, F., Godaux, E., Cordell, B., and Van Leuven, F. (1999) Early phenotypic changes in transgenic mice that overexpress different mutants of amyloid precursor protein in brain. *J. Biol. Chem. 274*, 6483−6492.

(5) Moechars, D., Lorent, K., and Van Leuven, F. (1999) Premature death in transgenic mice that overexpress a mutant amyloid precursor protein is preceded by severe neurodegeneration and apoptosis. *Neuroscience 91*, 819−830.

(6) Kumar-Singh, S., Dewachter, I., Moechars, D., Lubke, U., De Jonghe, C., Ceuterick, C., Checler, F., Naidu, A., Cordell, B., Cras, P., Van Broeckhoven, C., and Van Leuven, F. (2000) Behavioral disturbances without amyloid deposits in mice overexpressing human amyloid precursor protein with Flemish (A692G) or Dutch (E693Q) mutation. *Neurobiol. Dis. 7*, 9−22.

(7) Mucke, L., Masliah, E., Yu, G. Q., Mallory, M., Rockenstein, E. M., Tatsuno, G., Hu, K., Kholodenko, D., Johnson-Wood, K., and McConlogue, L. (2000) High-level neuronal expression of $A\beta_{1-42}$ in wild-type human amyloid protein precursor transgenic mice: Synaptotoxicity without plaque formation. *J. Neurosci. 20*, 4050−4058.

(8) Fancy, D. A., and Kodadek, T. (1999) Chemistry for the analysis of protein−protein interactions: Rapid and efficient cross-linking triggered by long wavelength light. *Proc. Natl. Acad. Sci. U. S. A. 96*, 6020−6024.

(9) Bitan, G., Kirkitadze, M. D., Lomakin, A., Vollers, S. S., Benedek, G. B., and Teplow, D. B. (2003) Amyloid β-protein (Aβ) assembly: Aβ40 and Aβ42 oligomerize through distinct pathways. *Proc. Natl. Acad. Sci. U. S. A. 100*, 330−335.

(10) Ono, K., Condron, M. M., and Teplow, D. B. (2009) Structure-neurotoxicity relationships of amyloid β-protein oligomers. *Proc. Natl. Acad. Sci. U. S. A. 106*, 14745−14750.

(11) Roychaudhuri, R., Yang, M., Hoshi, M. M., and Teplow, D. B. (2009) Amyloid β-protein assembly and Alzheimer disease. *J. Biol. Chem. 284*, 4749−4753.

(12) Lazo, N. D., Grant, M. A., Condron, M. C., Rigby, A. C., and Teplow, D. B. (2005) On the nucleation of amyloid β-protein monomer folding. *Protein Sci. 14*, 1581−1596.

(13) Maji, S. K., Ogorzalek Loo, R. R., Inayathullah, M., Spring, S. M., Vollers, S. S., Condron, M. M., Bitan, G., Loo, J. A., and Teplow, D. B. (2009) Amino acid position-specific contributions to amyloid β-protein oligomerization. *J. Biol. Chem. 284*, 23580−23591.

(14) Walsh, D. M., Hartley, D. M., Kusumoto, Y., Fezoui, Y., Condron, M. M., Lomakin, A., Benedek, G. B., Selkoe, D. J., and Teplow, D. B. (1999) Amyloid β-protein fibrillogenesis. Structure and biological activity of protofibrillar intermediates. *J. Biol. Chem. 274*, 25945−25952.

(15) Bitan, G., and Teplow, D. B. (2004) Rapid photochemical cross-linking–A new tool for studies of metastable, amyloidogenic protein assemblies. *Acc. Chem. Res. 37*, 357−364.

(16) Cleveland, D. W., Fischer, S. G., Kirschner, M. W., and Laemmli, U. K. (1977) Peptide mapping by limited proteolysis in sodium dodecyl sulfate and analysis by gel electrophoresis. *J. Biol. Chem. 252*, 1102−1106.

(17) Kirkitadze, M. D., Bitan, G., and Teplow, D. B. (2002) Paradigm shifts in Alzheimer's disease and other neurodegenerative disorders: The emerging role of oligomeric assemblies. *J. Neurosci. Res. 69*, 567−577.

(18) Klein, W. E. (2006) Cytotoxic intermediates in the fibrillation pathway: Aβ oligomers in Alzheimer's disease as a case study. In *Part A: Protein Misfolding, Aggregation, and Conformational Diseases* (Uversky, V. N., and Fink, A. L., Eds.) pp 61−75, Springer, New York.

(19) Bitan, G., Vollers, S. S., and Teplow, D. B. (2003) Elucidation of primary structure elements controlling early amyloid β-protein oligomerization. *J. Biol. Chem. 278*, 34882−34889.

(20) Bitan, G., Lomakin, A., and Teplow, D. B. (2001) Amyloid β-protein oligomerization: prenucleation interactions revealed by photo-induced cross-linking of unmodified proteins. *J. Biol. Chem. 276*, 35176−35184.

(21) Diociaiuti, M., Macchia, G., Paradisi, S., Frank, C., Camerini, S., Chistolini, P., Gaudiano, M. C., Petrucci, T. C., and Malchiodi-Albedi, F. (2014) Native metastable prefibrillar oligomers are the most neurotoxic species among amyloid aggregates. *Biochim. Biophys. Acta, Mol. Basis Dis. 1842*, 1622−1629.

(22) Meyer, J. P., Pelton, J. T., Hoflack, J., and Saudek, V. (1991) Solution structure of salmon calcitonin. *Biopolymers 31*, 233−241.

(23) Roychaudhuri, R., Yang, M., Deshpande, A., Cole, G. M., Frautschy, S., Lomakin, A., Benedek, G. B., and Teplow, D. B. (2013) C-terminal turn stability determines assembly differences between Aβ40 and Aβ42. *J. Mol. Biol. 425*, 292−308.

(24) Maji, S. K., Amsden, J. J., Rothschild, K. J., Condron, M. M., and Teplow, D. B. (2005) Conformational dynamics of amyloid β-protein assembly probed using intrinsic fluorescence. *Biochemistry 44*, 13365−13376.

(25) Urbanc, B., Betnel, M., Cruz, L., Bitan, G., and Teplow, D. B. (2010) Elucidation of amyloid β-protein oligomerization mechanisms: discrete molecular dynamics study. *J. Am. Chem. Soc. 132*, 4266−4280.

(26) Chen, W. T., Hong, C. J., Lin, Y. T., Chang, W. H., Huang, H. T., Liao, J. Y., Chang, Y. J., Hsieh, Y. F., Cheng, C. Y., Liu, H. C., Chen, Y. R., and Cheng, I. H. (2012) Amyloid-β (Aβ) D7H mutation increases oligomeric Aβ42 and alters properties of Aβ-zinc/copper assemblies. *PLoS One 7*, e35807.

(27) Sugiki, T., and Utsunomiya-Tate, N. (2013) Site-specific aspartic acid isomerization regulates self-assembly and neurotoxicity of amyloid-β. *Biochem. Biophys. Res. Commun. 441*, 493−498.

(28) Yang, M., and Teplow, D. B. (2008) Amyloid β-protein monomer folding: free-energy surfaces reveal alloform-specific differences. *J. Mol. Biol. 384*, 450−464.

(29) Oosawa, F., Asakura, S., and Ooi, T. (1961) Physical Chemistry of Muscle Protein "Actin". *Prog. Theor. Phys. Suppl. 17*, 14−34.

(30) Oosawa, F., and Kasai, M. (1962) A theory of linear and helical aggregations of macromolecules. *J. Mol. Biol. 4*, 10−21.

(31) Murray, M. M., Bernstein, S. L., Nyugen, V., Condron, M. M., Teplow, D. B., and Bowers, M. T. (2009) Amyloid β-protein: Aβ40 inhibits Aβ42 oligomerization. *J. Am. Chem. Soc. 131*, 6316−6317.

(32) Bernstein, S. L., Dupuis, N. F., Lazo, N. D., Wyttenbach, T., Condron, M. M., Bitan, G., Teplow, D. B., Shea, J. E., Ruotolo, B. T., Robinson, C. V., and Bowers, M. T. (2009) Amyloid-β protein oligomerization and the importance of tetramers and dodecamers in the aetiology of Alzheimer's disease. *Nat. Chem. 1*, 326−331.

DOI: 10.1021/acs.biochem.5b00318
Biochemistry 2015, 54, 5315−5321